Deterioration of Lesno Brdo limestone on monuments (Ljubljana, Slovenia)

Propadanje lesnobrdskega apnenca na objektih kulturne dediščine (Ljubljana, Slovenia)

Sabina Kramar[1, *], Ana Mladenović[2], Maja Urosevic[3], Alenka Mauko[2], Helmut Pristacz[4] & Breda Mirtič[5]

[1]Institute for the Protection of Cultural Heritage of Slovenia, Conservation Centre, Restoration Centre, Poljanska 40, SI-1000 Ljubljana, Slovenia
[2]Slovenian National Building and Civil Engineering Institute - ZAG Ljubljana, Dimičeva 12, SI-1000 Ljubljana, Slovenia
[3]University of Granada, Faculty of Science, Department of Mineralogy and Petrology,
Avda. Fuentenueva s/n, 18071 Granada, Spain
[4]University of Vienna, Institute of Mineralogy and Crystallography, Althanstrasse 14, 1090 Vienna, Austria
[5]University of Ljubljana, Faculty of Natural Sciences and Engineering, Department of Geology, Aškerčeva 12, SI-1000 Ljubljana, Slovenia

*Corresponding author. E-mail: sabina.kramar@rescen.si

Received: December 14, 2009 **Accepted:** February 2, 2010

Abstract: This study deals with the characterization of Lesno Brdo limestone, widely used in the construction of Slovenian historical monuments as well as modern buildings. Samples of this limestone were subjected to a detailed investigation, using a number of different techniques: optical microscopy, scanning electron microscopy with EDS, X-ray powder diffraction, analysis by ICP-ES, porosity accessible to water under vacuum, capillary absorption, mercury intrusion porosimetry, gas sorption and ultrasonic velocity measurements. The object of these tests was to determine the mineralogical and microstructural parameters which affect the durability of the investigated stone, whose main mineral component is calcite, although quartz, dolomite and phyllosilicates are also present. Very low values of porosity were measured, as well as slow capillary

Original scientific paper

kinetics. Pore size distribution was found to be variable, and anisotropy high. The deterioration of the limestone on two monuments, one of which had been exposed to an outdoor environment, and the other to an indoor environment, was studied. The results indicated that the precipitation of soluble salts had significantly contributed to the severe observed deterioration of the limestone.

Izvleček: Prispevek obravnava lesnobrdski apnenec, ki je bil široko uporabljen pri gradnji številnih objektov kulturne dediščine in prav tako pri gradnji modernih objektov. Vzorci apnenca so bili preiskani z optično mikroskopijo, elektronsko mikroskopijo z EDS, rentgensko praškovno difrakcijo in ICP-ES. Med fizikalno-mehanskimi lastnostmi so bile merjene poroznost, vpijanje vode, plinska adsorpcija in prehod vzdolžnih ultrazvočnih valov. Z naštetimi meritvami smo želeli ugotoviti, kateri mineraloški in mikrostrukturni parametri vplivajo na obstojnost apnenca. Apnenec poleg kalcita sestavljajo še dolomit, kremen in filosilikati. Rezultati so pokazali, da ima apnenec zelo nizko poroznost in kinetiko kapilarnega dviga. Nadalje je bil predmet preiskave ugotavljanje propadanja apnencev na objektih kulturne dediščine. Ugotovljeno je bilo, da je kristalizacija v vodi topnih soli eden izmed glavnih vzrokov propadanja.

Key words: limestone, weathering response, deterioration, soluble salts, historical monuments

Ključne besede: apnenec, obstojnost, propadanje, topne soli, kulturna dediščina

Introduction

The severity of stone deterioration depends on complex interactions between a number of environmental and intrinsic properties, as well as on the duration of exposure. In terms of mineralogy and structure, stone is an extremely complex material - a complexity that is reflected in its weathering response to the natural and the built environment.[1] Proper knowledge of the properties of stone and an understanding of deterioration factors and processes are necessary for successful maintenance, protection and suitable conservation-restoration interventions.

Since prehistoric times, limestone has been one of the most common types of building stone, with continued applications in present building works and in conservation practice as a replacement material for the reconstruction of monuments. Although limestone consists mainly of calcite, it can show significant variations in its minor mineral composition, as well as in its structure and texture, resulting in complex and contrasting weathering behaviour. Many sedimentary rocks contain clay that can cause swelling when the stone is exposed to moisture, resulting in damage to monuments.[2, 3] Among the parameters which influence stone deterioration, moisture and the movement of water through the pore network are very important. Damage due to the soluble salt crystallization is considered to be a common risk, which plays a major role in the decay of limestone. Such salts are known to cause damage to porous materials through a variety of mechanisms, such as the production of physical stress resulting from their crystallization in the pores, differential thermal expansion, hydration pressure and enhanced wet/dry cycling caused by deliquescent salts.[4, 5] The properties, behaviour and decay of limestones have been profusely studied over the last decade by means of different approaches, especially focusing on their characterization as building materials with respect to estimates of durability[6–11] and to the assessment of limestone decay on monuments.[12–17]. However, whereas these studies have been mainly concerned with porous limestones, detailed studies of the properties of compact limestones are still rare.[18–22]

Two lithotypes of a compact limestone from the Lesno Brdo quarry, which is located approximately 10 km west of Ljubljana, were selected for a detailed study of their properties and deterioration phenomena. This limestone, known as Lesno Brdo limestone, is characterized by various colours: red, pink, and all possible nuances from light to dark grey. It has been frequently employed in the construction of Slovenian historical monuments,[23, 24, 25] as well as in modern buildings. These colours are sometimes shot through each other, whereas they are sometimes clearly separated.[23, 24] The dark grey lithotype was selected because, in recent years, due to the geological conditions, it has become easier to extract and therefore more popular for use in the construction of modern buildings. The light red lithotype was selected not only because it is very decorative, and for this reason was frequently used in historical buildings and monuments, but also because in past centuries it was the leading lithotype from this quarry. It is still available today, in smaller quantities, and is used, for example, in contemporary buildings as cladding and flooring, or as replacement material in works for the conservation and restoration of historical monuments.

Thus, the two main aims of the investigation were: firstly, to characterize the light red and dark grey lithotypes of the Lesno Brdo limestone from the mineralogical, chemical and petrophysical points of view, and to assess the differences between the lithotypes with respect to their durability, and, secondly, to characterize the deterioration patterns of two historical monuments, made mainly using the red lithotype, one of which had been exposed to an outdoor environment, and the other to an indoor environment.

MATERIALS AND METHODS

Materials

Limestone was sampled in the local active quarry of Lesno Brdo near Ljubljana (Central Slovenia). Two lithotypes of Triassic reef limestone were selected for this study: the dark grey lithotype (these samples were labelled: SLB) and the light red lithotype (these samples were labelled: PLB).

Additionally, as a part of a broader conservation - restoration projects, sampling was also carried out on two baroque monuments, located in the old part of the city of Ljubljana, Slovenia: the Fountain of the Three Carniolian Rivers, commonly known as Robba's Fountain, which is shown in Figure 1a (the samples from this monument were designated: RO), which was constructed between 1743 and 1751, and one of the side altars in the Church of St. James, in the Chapel of St. Francis Xavier, which is shown in Figure 1b (the samples from this monument were designated: JAL), and was constructed between 1709 and 1722. The elements of the fountain consist of four different types of natural stone. The architectural part of the monument consists of two different types of Slovenian limestone and a conglomerate, whereas the three statues are sculpted out of Carrara marble. The light red lithotype of Lesno Brdo limestone was used for the construction of this monument's obelisk. The side altar in the Chapel of St. James' Church is made of 18 different types of natural stone, whereas both of the above-mentioned lithotypes of Lesno Brdo limestone were used for the construction of some of the lower parts of the altar. A total of 15 samples from the two considered monuments were carefully collected, paying special attention to the sampling the different textures of the weathering forms, and the degree of damage. Detailed information about the fresh and weathered samples is provided in Table 1.

Analytical methods

Polished thin sections of six samples of the limestone from the quarry (three per lithotype) were studied by optical microscopy, using an Olympus BX-60 equipped with a digital camera (Olympus JVC3-CCD).

The samples of both unweathered and weathered limestone were examined by a Scanning Electron Microscope

Figure 1. Selected monuments and weathering forms of Lesno Brdo limestone. (a) Fountain of the Three Carniolian Rivers - the obelisk is made of Lesno Brdo limestone, and the statues of Carrara marble. (b) Side altar of the Church of St. James. Some of the stone elements of the lower parts are made of Lesno Brdo limestone. (c) The black crusts are compact aggregates of salt minerals, occurring on the surface on sheltered areas. The Figure shows a detail of the obelisk of the Fountain. (d) Fluffy efflorescence, appearing as very loosely coherent aggregates of acicular and long hair-like crystals. The Figure shows a detail of the lower part of the altar. The width of the image is about 10 cm.

Table 1. Summary of the investigated samples, showing the related weathering forms and mineralogy as determined by X-ray powder diffraction and SEM-EDS

Unweathered samples			
Limestone	*Location*	*Investigated samples*	*Primary mineralogy*
Dark grey lithotype	Lesno Brdo quarry	SLBa, SLBb, SLBc	calcite, dolomite, quartz, clinochlore, muscovite/illite
Light red lithotype	Lesno Brdo quarry	PLBa, PLBb, PLBc	calcite, dolomite, quartz, clinochlore, muscovite/illite
Samples from monuments			
Weathering type	*Location*	*Investigated samples*	*Weathering products*
black crust	fountain	RO94, RO95, RO97, RO98, RO99, RO100	gypsum
flaking	fountain	RO94, RO95, RO97, RO98, RO99	gypsum
white crust	altar	JAL173, JAL175, JAL176	gypsum
flaking	altar	JAL173, JAL182	gypsum
subflorescence	altar	JAL173, JAL182	gypsum
crumbling	altar	JAL177, JAL184	gypsum
efflorescence	altar	JAL174, JAL180, JAL181	gypsum, nitre, hexahydrite, pentahydrite

(JEOL 5600 LV), using electron backscattering. Some particular areas of the samples were analyzed for chemical composition using an Energy Dispersive X-ray Spectrometer (EDS). The excitation voltage was 20 kV, and the pressure was between 10 Pa and 20 Pa.

The mineral composition of both the unweathered limestone and the weathering products was determined by X-ray powder diffraction, using a Philips PW3710 X-ray diffractometer equipped with Cu Kα radiation, and a secondary graphite monochromator. The samples were milled in an agate mortar to a particle size of less than 50 μm. The data were collected at 40 kV and a current of 30 mA, in the range from $2\theta = (2 \text{ to } 70)^{\circ}$. Afterwards, each sample of limestone was treated in order to extract its acid-insoluble residue. About 400 mg of each sample was crushed and dissolved in 20 mL of dilute HCl (1:10)[21]. The residue was then washed with distilled water in order to remove all traces of HCl. The acid-insoluble fraction was then analyzed using X-ray powder diffraction.

All the samples of the unweathered limestone were analyzed for their major chemical composition in an accredited commercial Canadian laboratory (Acme Analytical Laboratories, Vancouver, B.C., Canada), using different analytical methods. According to the results of the reports, SiO_2, Al_2O_3, Fe_2O_3, MgO, CaO, Na_2O, K_2O, TiO_2 and P_2O_5 were measured after fusion with a mixture of lithium metaborate/tetraborate and dissolution in nitric acid by inductively coupled plasma emission spectroscopy (ICP-ES). The total carbon content was obtained by combustion in an oxygen current (LECO method) and the CO_2 and volatile contents by precision scale weighing after calcination at 1100 °C (LOI). The accuracy and precision of the sample analyses were assessed by using the reference material CCRMR SO-18 CSC.

The total porosity (N_t) of the samples of unweathered limestone (three samples of (50 × 50 × 50) mm per lithotype) was measured by water uptake under a vacuum, according to the RILEM recommendations - RILEM I.1 Norm.[26] The water absorption coefficient (A/(g m^{-2} s$^{-1/2}$) was measured according to the RILEM II.6 Norm.[26]

The pore systems of the samples of unweathered limestone (three samples per lithotype) were further characterized by means of mercury intrusion porosimetry (MIP) and gas sorption isotherms. Small blocks, of size approximately 2 cm^3, were dried in an oven for 24 h at 60 ºC, and analyzed on a Micromeritics Autopore III model 9410 porosimeter. Adsorption and desorption isotherms of argon were obtained at –196 ºC on a Micromeritics Tristar 3000 Analyzer. In rock materials several fluids can be applied as adsorbates the most commonly used being nitrogen. However, in samples with a surface area of less than 5 m^2 g^{-1}, argon adsorption measurements are more accurate than when using nitrogen, which usually yield excessively high values.[27] Prior to measurement, samples were heated at 250 °C for 8 h, and outgassed to 1.33 × 10^{-3} mbar using Micromeritics Flowprep equipment. Gas adsorption analysis in the relative pressure range of 0.05 to 0.3 was used to determine the total specific area – BET surface area of the samples.[28, 29] The BJH method was used to obtain pore size distribution curves, the pore volume and the mean pore size of the rock samples.[30]

Ultrasonic velocity measurements (USV) were applied in order to demonstrate the homogeneity of the limestone. These measurements were performed using an AU 2000 Ultrasonic Tester (CEBTP), with transmission frequency of 60 kHz. The pulse propagation velocity was measured on dry test samples (three samples per lithotype, of size: (50 × 50 × 50) mm). Three measurements were performed in each of the three orthogonal directions. Additionally, the total structural anisotropy coefficient ΔM/% and the relative anisotropy coefficient Δm/% of the stone material were obtained from the mathematical relations between the ultrasonic propagation velocities, following the equations of Guydader and Denis.[31]

Results and discussion

Characterization of samples from the quarry

Mineral and chemical composition

Petrographical analysis indicated that the limestone is very heterogeneous, being classified as mainly micritic with a transition to microsparitic (Figures 2a and 2b). Intraclasts, pellets and fragments of fossils (mainly red algae and shells) are present in both lithotypes. The light red lithotype is slightly more heterogeneous, due to the presence of numerous veins and styloliths. The styloliths are filled either with phyllosilicates (minerals of the chlorite and mica groups) and iron oxides/hydroxides or dolomite. Calcite occurs mainly as micrite, but also as sparitic crystals in veins, and as fragments of shells. Some parts of both lithotypes consist of coarse-grained dolomite crystals with sizes up to 2 mm, which are sometimes partly or completely replaced by calcite. Iron oxides/hydroxides occur in the calcitic rims of the coarse-grained dolomite. These could be clearly observed by SEM-EDS (Figure 2c), which revealed that the rims of the coarse-grained crystals of dolomite are partially replaced by calcite. The iron oxides/hydroxides occur macroscopically as a brown colour, enclosing the dolomite. The intergranular spaces of the coarse-grained dolomite and calcite are mainly filled with phyllosilicates, as was proved by SEM-EDS analysis (Figure 2c). According to the results of EDS, the chemical composition of the material in the intergranular spaces consists of K-rich alumosilicates, which are assumed to be sericite (fine grained muscovite). In some veins the intergrowing of sericite with clinochlore can be observed, as can be seen in Figure 2d. Homogenously distributed, single grains of ilmenite and apatite commonly occur in veins of phyllosilicates. Quartz occurs as autogenous or as terrigenous grains. It can also occur in veins, as polycrystallinic quartz. SEM-EDS analysis of the limestone samples also confirmed the occurrence of quartz grains, which are homogeneously distributed over the sample.

The results of the X-ray powder diffraction analysis (Table 1) of the bulk limestone indicate that calcite, as well as dolomite and quartz, are present in all the samples. Phyllosilicates such as clinochlore and muscovite/illite were detected in all three samples of the light red lithotype, but only in one sample of the dark grey lithotype (SLBa). X-ray

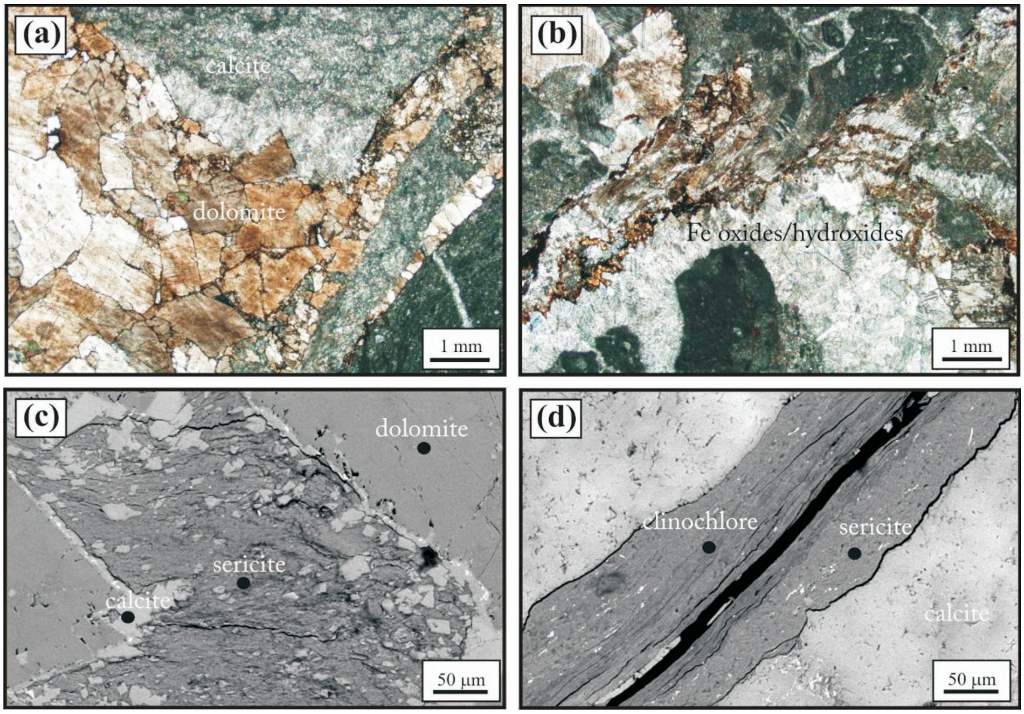

Figure 2. Microimages of Lesno Brdo limestone. (a) The dark grey lithotype. The image shows coarse-grained dolomite, surrounded by sparitic and micrite calcite. Transmitted light, parallel polars. (b) The light red lithotype. The image shows a very heterogeneous structure, with brownish veins of Fe oxides/hydroxides and clay. Transmitted light, parallel polars. (c) An SEM-BSE image of an intergranular space, filled with sericite. Fe oxides/hydroxides are present in the calcitic rims of the coarse-grained dolomite. (d) The SEM-BSE image show the intergrowing of sericite (brighter areas) with clinochlore (darker areas). The small bright areas indicate the presence of ilmenite.

Table 2. Bulk chemical composition of the limestone samples, determined by ICP-ES. All the oxides, as well as the loss on ignition - LOI and the total carbon - TOT/C, are given in mass fractions *w*/%

Samples	SiO_2	Al_2O_3	Fe_2O_3	MgO	CaO	Na_2O	K_2O	TiO_2	P_2O_5	LOI	TOT/C
SLBa	2.41	1.50	0.24	1.26	53.71	0.04	0.36	0.05	0.02	35.2	12.12
SLBb	0.92	0.35	0.05	0.59	56.27	0.02	0.08	0.01	<0.01	35.5	12.06
SLBc	0.91	0.45	0.11	3.64	50.88	0.04	0.10	0.01	<0.01	43.8	12.39
PLBa	5.73	3.41	0.79	0.90	52.47	0.06	0.80	0.10	0.02	35.7	10.92
PLBb	5.31	3.32	0.45	1.70	62.63	0.14	0.64	0.11	0.02	35.6	10.95
PLBc	2.96	1.54	0.53	2.96	51.62	0.02	0.33	0.04	0.01	36.2	12.01

powder diffraction analysis of the acid-insoluble residue likewise revealed the presence of quartz, muscovite/illite and clinochlore, as minor components. All samples of the light red lithotype consisted of muscovite/illite, clinochlore and quartz, whereas the acid-insoluble residue in the dark grey lithotype represents quartz, and only in one sample muscovite/illite and clinochlore. Due to the small quantities of ilmenite and apatite, it was not possible to detect these minerals using this method.

The results of bulk chemical analyses of all of the investigated samples are given in Table 2. They reveal high heterogeneity in the chemical and thus also mineralogical composition of the samples. In all the samples CaO is invariably the main chemical component, indicating that the limestone is mainly composed of calcite. The light red lithotype of limestone has a higher content of SiO_2, Al_2O_3, Fe_2O_3 and K_2O, thus reflecting the presence of phyllosilicates and quartz. K_2O indicates the presence of muscovite/illite, whereas the high fraction of the MgO component indicates the presence of dolomite and clinochlore. High contents of Fe_2O_3 indicate the presence of clinochlore and iron oxides/hydroxides in the veins. The contents of TiO_2 and P_2O_5 are higher in the samples of the light red lithotype, which can be attributed to the presence of ilmenite and apatite in sericite and clinochlore-rich veins.

Physical and mechanical properties

As water plays a fundamental role in stone deterioration, the properties of the stone structure and water transfer were measured. It is well known that water is one of the most important deterioration agents, and also facilitates the damaging action of other agents, such as salts. The petrophysical characteristics of the limestone are shown in Table 3. All the samples have low porosity, which is less than 1 % by mass, determined by the water vacuum method. The coefficient of capillarity is rather low, too. The average values were (0.24 ± 0.03) g m^{-2} $s^{-0.5}$ for the light red lithotype, and (0.09 ± 0.05) g m^{-2} $s^{-0.5}$ for the dark grey lithotype. The obtained values are of the same order of magnitude as for some other limestones.[18] The light red limestone exhibited slighter higher values of porosity, which is also reflected in the high water absorption coefficient. This behaviour may be explained by the presence of veins filled with clay minerals, which are more abundant in the light red lithotype.

Pore size distribution is important for understanding the movement of fluids inside the pore structure. It is well-known that different pore size can result in different behaviours relative to water.[17] Pores are classified into three types,[32] as follows: a) pores smaller than 0.1 μm, in which capillary condensation takes place; b) pores in the size range from 0.1 μm to 5.0 μm, in which water transport mechanism is capillary suction and c) pores larger than 5.0 µm, the range of pores allowing free water to penetrate the porous material. The pore volume and pore size distribution between 0.003 µm and 100 µm (radius) were measured by mercury intrusion porosimetry. The results of two studied lithotypes are shown in Table 3. The light red lithotype of limestone is more porous than the dark grey lithotype, with open porosity values of (2.49 ± 0.97) % vs. (1.60 ± 0.76) % respectively, even though the bulk density of both lithotypes is almost the same.

When considering damage due to salt crystallization, the critical pore radius where the crystallization pressure is effective ranges below 0.05 µm.[33] The gas-physisorption method is thus suitable for investigation of this range of pore radii. Scherer[34] established that the maximum pressure that salt crystallization can achieve is highly dependent on the size of the pores, predicting that most of the damage occurs when salt-rich fluids migrate from pores of larger size to pores of smaller size, in the range between 4 nm and 50 nm. Pore size distribution thus controls the

Table 3. Physical and mechanical properties of the limestone. The pore system characteristics were determined by the water vacuum method, water absorption, Hg porosimetry and Ar sorption. Average values of ultrasound velocities, measured in three orthogonal directions (V_1, V_2, V_3), structural anisotropy (ΔM) and relative anisotropy (Δm).

Method of investigation	SLB	PLB
Porosity accessible to water (%)	0.18 ± 0.04	0.25 ± 0.03
Coefficient of capillarity (g m^{-2} s$^{-0,5}$)	0.16 ± 0.03	0.24 ± 0.03
Hg porosimetry		
Open porosity (%)	1.60 ± 0.76	2.49 ± 0.97
Apparent density (g cm^{-3})	2.74 ± 0.01	2.76 ± 0.01
Bulk density (g cm^{-3})	2.69 ± 0.03	2.68 ± 0.03
Ar adsorption		
Surface area (m^2/g)	0.0979 ± 0.0056	0.3787 ± 0.0668
Total pore volume (cm^3/g)	0.00011 ± 0.00001	0.00034 ± 0.00010
Average pore diameter (nm)	2.093 ± 0.021	2.114 ± 0.002
Ultrasound velocity measurements		
V_1/(km/s)	5.20 ± 0.17	4.95 ± 0.25
V_2/(km/s)	5.04 ± 0.09	4.76 ± 0.22
V_3/(km/s)	4.94 ± 0.14	4.41 ± 0.03
ΔM/%	3.50 ± 1.44	9.06 ± 3.72
Δm/%	3.10 ± 2.25	7.99 ± 3.85

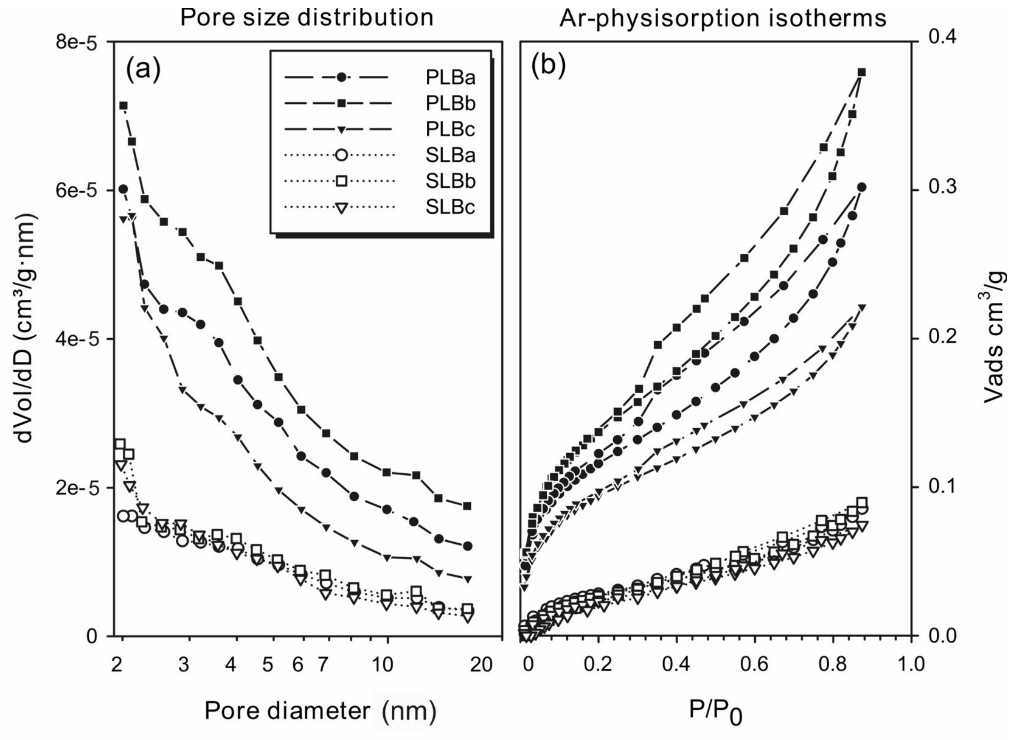

Figure 3. Results of BET measurements. (a) The volume of pores accessible to BET is significant higher for the light red lithotype than for the dark grey lithotype. (b) The Ar-physisorption isotherms for both lithotypes.

crystallization pressure. Table 3 shows that the light red lithotype has, in general, a higher BET surface area, as well as a higher average pore size, than the dark grey lithotype. The differences in pore size distribution between the two lithotypes can be seen in Figure 3a. The volume of pores accessible to gas is larger and much more variable in the case of the light red lithotype. Similarly to previous results, the higher BET surface area in the light red lithotype is the result of the presence of discontinuities filled with clay minerals. Furthermore, the Ar-physisorption isotherm is steeper, and indicates a more complex and variable pore system in the case of the samples of the light red lithotype (see Figure 3b). To the contrary, the samples of the dark grey lithotype are very homogeneous in terms of their pore size distribution (Figure 3a), as well as the complexity of the pore system network (Figure 3b). All studied samples have a physisorption isotherm of type II, which is characteristic for non-porous or macroporous materials,[27] which is confirmed by the very low surface area in both lithotypes (Table 3). Furthermore, in the case of the samples of the light red lithotype, a H3 type of hysteresis loop can be recognised, with non-limited adsorption at high relative pressures and with forced closure of the hysteresis loop in the desorption branch around relative pressure of 0.4. Such a type of hysteresis loop is characteristic for materials with slit-shaped pores.[35]

Ultrasonic measurements can be used indirectly to define textural properties and, therefore, also physical-mechanical properties.[32] The results of the ultrasonic velocity measurements are listed in Table 3. Samples of the dark grey lithotype revealed faster ultrasonic wave propagation, indicating greater compactness and higher mechanical resistance when compared with the light red lithotype. Furthermore, the total structural anisotropy (ΔM) and relative structural anisotropy (Δm) are lower in the case of the dark grey lithotype, suggesting its higher compactness. On the contrary, the anisotropy is higher in case of the light red lithotype, as it is more heterogenous due to the more frequent appearance of discontinuities. An increase in the anisotropy of the samples is observed in case of the occurrence of bigger piles or veins of coarse-grained dolomite, calcitic veins, fissures and styllolithes in the samples. The values are in accordance with the obtained values of the porosity, as porosity decreases exponentially with velocity. Water transfer properties are directly linked to the pore network. The higher porosity and the high imbibition coefficient in the light red lithotype imply that water moves easily, and that the water transfer induces various physical-chemical reactions that eventually lead to deterioration of investigated limestone.

Limestone deterioration

Weathering forms on monuments

Within the framework of broader conservation - restoration projects, in situ investigations of the monuments by means of monument mapping was pointed out several types of deterioration phenomena. The studied limestone deteriorates extensively when subjected to either an outdoor or an indoor environment. A wide range of different weathering forms, documented according to the Fitzner classification [36] was observed. Crumbling, flaking and black crust are present on the limestone parts of the outdoor monument, whereas flaking, subflorescence, crumbling, white crust and efflorescence are present on the indoor monument. Examples of weathering forms are shown in Figure 1c and Figure 1d.

Weathering products and mechanisms

X-ray diffraction data (Table 1), supported by the results of SEM-EDS examinations, have shown that soluble salts are the main weathering products. Almost all weathering forms are related to salt crystallization, as seen in Figure 3.

The black crusts outdoor, as well the white crusts indoor, were composed of gypsum. The crusts are generally formed by less soluble salts, as gypsum.[37] The black crusts consists of gypsum crystals up to 100 μm in size, which are oriented parallel to the surface (Figures 4a, 4b and 4c). In some places individual calcite grains are enclosed in the gypsum crystals. Ba-rich (Figure 4d) or Fe-rich aerosols have been documented between the gypsum crystals of the crust, pointing to the effect of air pollutants. The boundary between the gypsum and the limestone is extremely irregular, showing progressive chemical dissolution of the calcite grains. Some of the white crusts occurring under indoor conditions (Figure 4e, with a thickness of 30 μm to 200 μm) show several alternating layers of columnar crystals. This suggests rhythmic fluctuations in the solution supply. Moreover, the salt crystals of gypsum are oriented perpendicularly to the surface of the limestone. Although the origin and growth of the sulphated crusts have been widely studied in the past,[38–43] literature data are still not uniform either the crust formation is actually a deleterious process, as rainwater arrives at the boundaries between the gypsum and the limestone where transformation of the calcite into gypsum occurs or that gypsum formation result in passivation on the surface of limestone, which might prevent further deterioration.

Salt crystallization under the surface (subflorescence) or within the pores resulted in disruption of the limestone (Figure 4f), expressed as flaking and crumbling of the limestone under both outdoor and indoor conditions. As the crystals exceed the size of the original pores, pressures strong enough to disrupt the fabric are built up by the growing crystals. These flakes are about 200 μm wide, and around 50 μm thick. The system of fissures is present 100 μm to 150 μm beneath the surface, whereas the fissures are 20 μm to 30 μm thick. Apparently, in some cases gypsum crystals nucleate in veins of clay minerals, as can be seen in Figure 4g, which are more accessible to porous flow. As salts concentrate in those parts which retain moisture longer, the swelling clay minerals enhance the salt-related breakdown. Moreover, the cyclic swelling and shrinking of clay contribute to the additional delamination of the limestone.[9, 44] Flaking of the limestone is not merely concentrated to the areas of clay-rich veins, as subflorescence in limestone occurs when the capillary flux is slower than the evaporation flux.[45] Water transfer is, due to the low porosity of the limestone, decreased, resulting in higher evaporation from the limestone surface with regard to the velocity of the capillary flux. Thus, this zone is mechanically stressed, leading to disrupture of the limestone.

Efflorescences (Figures 4h and 4i) are composed of magnesium sulphate hydrates (hexahydrite, pentahydrite), gypsum and nitre, as proved by X-ray powder diffraction and SEM-EDS observations. Three different mineral assemblages have been observed in the efflorescences: (1) nitre and gypsum, (2) nitre, gypsum and magnesium sulphate hydrates, or (3) gypsum and

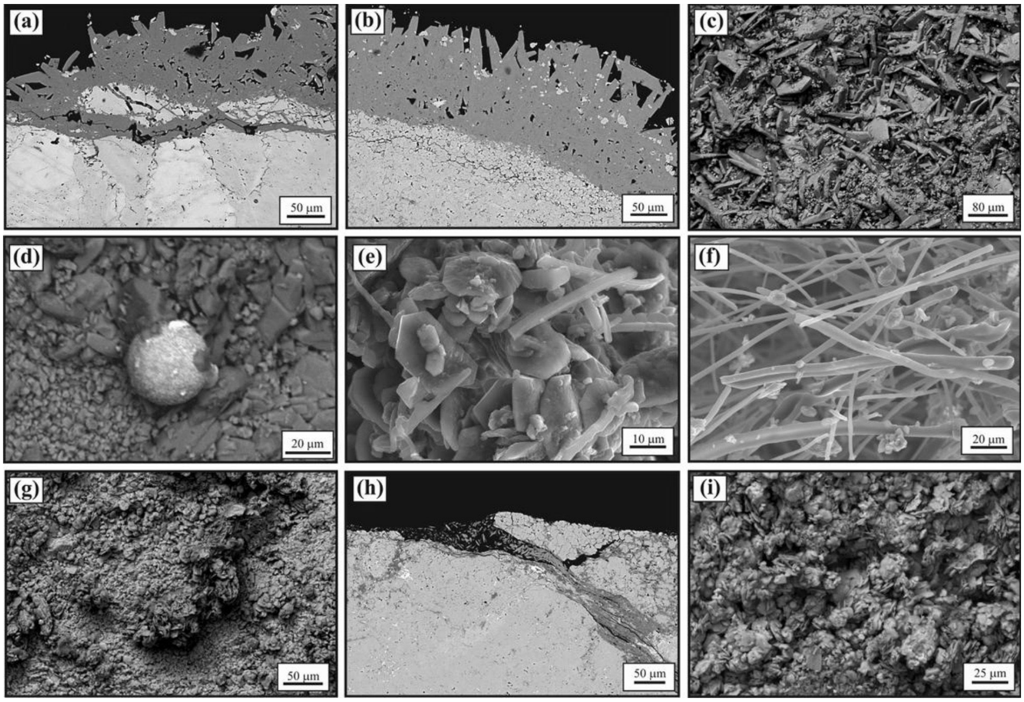

Figure 4. Microimages of deterioration patterns of the studied limestone. (a) Dissolution of calcite crystals under the gypsum crust, outdoors. On samples taken outdoors the dissolution of sparitic crystals under the gypsum crust is clearly evident. (b) Dissolution and disintegration of calcite crystals under the gypsum crust. Entrapped calcite grains in the crusts, outdoors. (c) Crystals of gypsum at the surface of the black crusts. d) A Ba-rich aerosol, entrapped between the gypsum crystals. (e) A white crust with gypsum crystals. (f) Gypsum filling the pores of the limestone leading to flaking of the limestone. (g) Gypsum crystallization in a vein of clay, which leads to flaking of the limestone, indoors. (h) Platy crystals of gypsum and elongated crystals of magnesium sulphate hydrates, indoors. (i) Fibrous crystals of nitre and platy crystals of gypsum, outdoors.

magnesium sulphate hydrates. Efflorescences appear as very loosely coherent aggregates of long hair-like needles and fibres (whisker growth), suggesting low supersaturation and a slightly humid to nearly dry surface substrate, where crystals grow on a solution film into the air.[46] Magnesium sulphates hydrates and nitre occur only on the surface of the limestone exposed to the indoor environment, due to their high solubility, whereas in the case of outdoor conditions they are not present. It has to be considered that the behaviour of multi component salt mixtures is extremely complex. It has been reported that, in normal outdoor environmental conditions, most salt remains in solution, except the rather insoluble gypsum that crystallizes out of the solution first.[4, 47] With the exception of hexahydrite–epsomite, transformations between the various species of the $MgSO_4 \times nH_2O$ series involve more than the simple removal of water: they require significant rearrangement of the crystal structure and the overcoming of activation energy barriers. Close to room temperature epsomite is the stable form in the presence of liquid water. Under dry conditions epsomite can dehydrate to form hexahydrite, and finally monohydrate kieserite.[48] The salt species that grow in efflorescences depend on the composition of the salt solution, on the properties of the substrate and on the environmental conditions during growth.[49] As joint mortars between the stone elements of the altar contain high quantities of soluble calcium and magnesium, are thus considered as potential source of these damaging salts. The contribution of nitre is significant in the samples taken from the stone elements at the bottom of the altar. The presence of nitre in those parts of the stone where there is a high capillary rise can be attributed to the solutions containing alkali potassium and nitrate that are present in the ground[50] or, alternatively, to the result of weathering due to K-bearing phyllosilicates.

Conclusions

The two lithotypes differ in their chemical composition and consequently in their mineralogy. Hence the other properties which are related to the mineral composition and their occurrence in the limestone also differ. The higher content of phyllosilicates is a remarkable feature of the light red lithotype. The porosity and values of the water transfer kinetics are very low for both lithotype, but they are slightly higher in the light red lithotype. The volume of pores accessible to gas is higher and much more variable for the light red lithotype, too. Furthermore, the Ar-physisorption isotherm is steeper and indicates a more complex and variable pore system of the light red lithotype. There were measurable differences in the USV measurements between the two lithotypes, showing higher anisotropy in the light red lithoytpe.

Limestone was found to be extensively deteriorated in both outdoor and indoor environments in the studied historical monuments, showing flaking, subflorescence, efflorescences, crumbling, and black and white crusts as deterioration phenomena. The results revealed that crystallization of soluble salts is the main weathering mechanism. Due to changeable environmental conditions, the soluble salts occurred in different varieties. Gypsum occurs as a compact crust, efflorescence and subflorescence, whereas magnesium sulphate hydrates and nitre crystallize only as efflorescence. Crystallization of gypsum under the surface resulted in flaking of the limestone. Furthermore, the presence of clay is also one of the main factors responsible for limestone deterioration, as a differential decay concentrated within the clay-rich planes resulting in the crumbling and formation of flakes.

The results presented here show that Lesno Brdo limestone, although compact, is relatively prone to deterioration. The presence of phyllosilicates indicates higher porosity and a higher imbibition coefficient than in the case of limestone not containing phyllosilicates, implying that, in the investigated limestone, water can move relatively easily, inducing physical-chemical reactions leading to its deterioration. The observed condition of the investigated historical monuments indicates that the presence of salts can be deleterious even to compact stone.

Acknowledgements

This research has been supported financially by the Slovenian Research Agency, under contract number 3211-05-000545. M. Urosevic received support in the form of a fellowship from the Spanish Ministry of Science (AP2006-036). Experimental support was provided by the Institute of Mineralogy and Crystallography, University in Vienna, and is hereby gratefully acknowledged. The authors also are grateful to Jože Drešar for performing the necessary sampling works on the selected monuments. Many thanks are due to José Alberto Padrón Navarta, for his helpful comments, and to Peter Sheppard for help with the editing of the text. The photographs shown in Figure 1a, 1b and 1 c are included by kind permission of Valentin Benedik.

References

[1] Warke, P. A., McKinley, J., Smith, B. J. (2006): Weathering of building stone: approaches to assessment, prediction and modelling. In: Kourkoulis S. K. editor. Fracture and Failure of Natural Building Stones. Springer, p. 313–327.

[2] Rodríguez-Navarro, C. E., Hansen, E., Sebastian, E., Ginell, W. S. (1997): The role of clays in the decay of ancient Egyptian limestone sculptures. *Journal of the Institute of American Conservators*, 36 (2), 151–163.

[3] Sebastián, E., Cultrone, G., Benavente, D., Linares Fernández, L., Elert, K., Rodríguez Navarro, C. (2008): Swelling damage in clay-rich sandstones used in the church of San Mateo in Tarifa (Spain). *Journal of Cultural Heritage*, 9, 66-76.

[4] Charola, E. A. (2000). Salts in the deterioration of porous materials: an overview. *Journal of the Institute of American Conservators*, 39, 327–343.

[5] Doehne, E. (2002): *Salt weathering: a selective review.* In: Siegesmund S, Weiss T, Vollbrecht A. editors. Natural stone, weathering phenomena, conservation strategies and case studies. Geological Society. London. Special Publication 205, p. 51–64.

[6] Colston, B. J, Watt, D. S, Munro, H. L.: Environmentally-induced stone decay: the cumulative effects of crystallization-hydration cycles on a Lincolnshire oopelsparite limestone. Journal of Cultural Heritage 2001; 4; 297–307.

[7] Selwitz, C., Doehne, E. (2002): The evaluation of crystallization modifiers for controlling salt damage to limestone. *Journal of Cultural Heritage*, 3, 205–216.

[8] Benavente, D., Garcià del Cura, M. A., Fort, R., Ordóñez, S. (2004): Durability estimation of porous building stones from pores structures and strength. *Engineering Geology*, 74, 113–127.

[9] Ruiz-Agudo, E., Mees, F., Jacobs, P., Rodriguez-Navarro, C. E. (2007): The role of saline solution properties on porous limestone salt weathering by magnesium and sodium sulfates. *Environmental Geology*, 52, 269–281.

[10] Cultrone, G., Russo L. G., Calabrò, C., Uroševič, M., Pezzino, A. (2008): Influence of pore system characteristics on limestone vulnerability: a laboratory study. *Environmental Geology*, 54, 1271–1281.

[11] Cardell, C., Benavente, D., Rodríguez-Gordillo, J. (2008): Weathering of limestone building material by mixed sulfate solutions. Characterization of stone microstructure, reaction products and decay forms. *Materials Characterization,* 59, 1371–1385.

[12] Tuğrul, A., Zarif, I. H.(1999): Research on limestone decay in a polluting environment, Istanbul-Turkey. *Environmental Geology,* 38, 149–158.

[13] Maravelaki-Kalaitzaki, P., Biscontin, G. (1999) Origin, characteristics and morphology of weathering crusts on Istria stone in Venice. *Atmospheric Environment*, 33, 1699–1709.

[14] Fitzner, B., Heinrichs, K., La Bouchardiere, D. (2002): Limestone weathering of historical monuments in Cairo, Egypt. In: Siegesmund S, Weiss T, Vollbrecht A, editors. Natural stone, weathering phenomena, conservation strategies and case studies. Geological Society; Special Publication 205, p. 217–239.

[15] Smith, B. J., Török, Á., McAlister, J.

J., Megarry, Y. (2003): Observations on the factors influencing stability of building stones following contour scaling: a case study of oolithic milestones from Budapest, Hungary. *Building and Environment*, 38, 1173–1183.

[16] Cardell, C., Celalieux, F., Roumpopoulos, K., Moropoulou, A., Auger, F., Van Grieken, R. (2003): Salt induced decay in calcareous stone monuments and buildings in a marine environment in SW France. *Construction and Building Materials*, 17, 165–179.

[17] Beck, K., Rozenbaum, O., Al-Mukhtar, M., Plançon, A. (2004): *Multiscale characterization of monument limestones.* In: Aires-Barros L, Zezza F, Editors. Proceedings of the 6th International Symposium on the conservation of Monuments in the Mediterranean Basin. Lisbon, p. 229–232.

[18] Sahlin, T., Malaga-Starzec, K., Stigh, J., Schouenborg, B. (2000): *Physical properties and durability of fresh and impregnated limestone and sandstone from central Sweden used for thin stone flooring and cladding.* In: Fassina V, editor. Proceedings of 9th International congress on deterioration and conservation of stone. Venice, p. 181–186.

[19] Nicholson, D. T. (2001): Pores properties as indicators of breakdown mechanisms in experimentally weathered limestones. *Earth Surface Processes and Landforms*, 26; 819–838.

[20] Török, Á. (2006): Influence of fabric on the physical properties of limestones, In: Kourkoulis S. K. editor. *Fracture and failure of Natural Building stones*, p. 487–495.

[21] Marszałek, M. (2007). *The mineralogical and chemical methods in investigations of decay of the Devonian Black »marble« from Dębnik (Southern Poland)*. In: Přikryl R, Smith B.J. editors. Building Stone Decay: From Diagnosis to Conservation. Geological Society. Special Publications 271, p. 109–115.

[22] Lindqvist, J. E., Malaga, K., Middendorf, B., Savukoski, M., Pétursson, P.: Frost resistance of Natural stone, the importance of micro- and nano-porosity, Geological Survey of Sweden External research project report, published online at: http://www.sgu.se/dokument/fou_extern/Lindqvist-et-al_2007.pdf.

[23] Mirtič, B., Mladenović, A., Ramovš, A., Senegačnik, A., Vesel, J., Vižintin, N. (1999): Slovenski naravni kamen. Geological Survey of Slovenia; Ljubljana; 1999.

[24] Ramovš, A. (2000): Podpeški in črni ter pisani lesnobrdski apnenec skozi čas. Mineral; Ljubljana.

[25] Jarc, S. (2000): Vrednotenje kemične in mineralne sestave apnencev kot naravnega kamna, Master Thesis, University of Ljubljana, Faculty of Natural Sciences and Engineering, Department of Geology, Ljubljana.

[26] RILEM, Recommended tests to measure the deterioration of stone and to assess the effectiveness of treatment

methods. Materials and Structures 1980; 14; 175–253.

[27] Sing, K. S. W., Everett, D. H., Haul, R. A. W., Moscou, L., Pierotti, R. A., Rouquérol, J., Siemieniewska, T. (1985): Reporting Physisorption Data for Gas/Solid Systems. Pure Applied Chemistry (IUPAC), 57, 603–619.

[28] Gregg, S. J., Sing, K. S. W. (1982): Adsorption Surface Area and Porosity. Academic Press; London.

[29] Adamson, A.W., Gast, A. P. (1997): Physical Chemistry of Surfaces. J.Wiley & Sons; New York.

[30] Barret, E. P., Joyner, L. G., Halenda, P. P. (1951): The Determination of Pore Volume and Area Distributions in Porous Substances. I. Computations from Nitrogen Isotherms, *Journal of the American Chemical Society*, 73, 373–380.

[31] Guydader, J., Denis, J. A. (1986): Propagation des ondes dans les roches anisotropes sous contrainte évaluation de la qualité des schistes ardoisiers. *Bulletin of the Engineering Geology*, 33, 49–55.

[32] Bourgès, A. (2006): Holistic correlation of physical and mechanical properties of selected natural stones for assessing durability and weathering. Ph. D. Thesis. München.

[33] Steiger, M. (2005): Crystal growth in porous materials II: Influence of crystal size on the crystallization pressure. *Journal of Crystal Growth*, 282, 470–481.

[34] Scherer, G. W. (1999): Crystallization in pores. *Cement and Concrete Research*, 29, 1347–1358.

[35] Lowell, S., Shields, J. E., Thomas, M. A., Thommes, M. (2004): Characterization of porous solids and powders: surface area, pore size and density. Springer.

[36] Fitzner, B., Heinrichs, K. (2002): *Damage diagnosis on stone monuments-weathering forms, damage categories and damage indices*. In: Prikryl R, Viles HA editors. Understanding and managing stone decay, Proceeding of the International Conference "Stone weathering and atmospheric pollution network (SWAPNET 2001)". Charles University in Prague. The Karolinum Press, p. 11–56.

[37] Arnold, A., Kueng, A. (1985): Crystallization and habits of salt efflorescences on walls, I., Methods of investigation and habits. In: Felix G, editor. Proceedings of the Fifth International Congress on the Deterioration and Conservation of Stone, Laussane: Presses Polytechniques Remandes, p. 255–67.

[38] Camuffo, D., Del Monte, M., Sabbioni, C. (1983): Origin and growth mechanisms of the sulphated crusts on urban limestone. *Water, Air, and Soil Pollution*, 19; 351–359.

[39] Ausset, P., Lefèvre, R. A. (2000): Early mechanisms of development of sulfated black crusts on carbonate stone. In: Fassina V, editor. Proceedings of the 9th International Congress on Deterioration and Conservation of Stone. Venice, p. 265–273.

[40] Gaviño, M., Hermosin, B., Verges-Belmin, V., Nowik, W., Saiz-Jimen-

ez, C. C. (2004): Composition of the black crusts from the Saint Denis Basilica, France, as revealed by gas chromatographymass pectroscopy. *Journal of Separation Science*, 27; 513–523.

41] Potgieter-Vermaak, S. S., Godoi, R. H. M., Van Grieken, R., Potgieter, J. H., Oujja, M., Catillejo, M. (2005): Micro-structural characterization of black crusts and laser cleaning of building stones by micro-Raman and SEM techniques. *Spectrochimica Acta. Part A*, 61, 2460–2467.

[42] Vazques-Calvo, C., Alvarez de Buergo, M., Fort, R., Varass, M. J. (2007): Characterization of patinas by means of microscopic techniques. *Materials Characterization*, 58, 1119–1132.

[43] Antill, S. J., Viles, H. A. (2003): Examples of the use of computer simulation as a tool for stone weathering research. Building and Environment, 38, 1243–1250.

[44] Rodriguez-Navarro, C., Sebastian, E., Doehne, E., Ginell, W. S. (1998): The role of sepiolite-palygorskite in the decay of ancient Egyptian limestone sculptures. *Clays and Clay Minerals*, 46 (4), 414–422.

[45] Lewin, S. Z. (1982): The Mechanism of Masonry Decay through Crystallization. In: Baer NS, editor. Conservation of Historic Stone Buildings and Monuments. National Academic Press; Washington DC, p. 120–144.

[46] Zehnder, K., Arnold, A. (1989): Crystal growth in salt efflorescence, *Journal of Crystal Growth*, 8, 513-521.

[47] Charola, E. A., Pühringer, J., Steiger, M. (2007): Gypsum: a review of its role in the deterioration of building materials. Environmental Geology, 52, 339–352.

[48] Juling, H., Kirchner, D., Brüggerhof, S., Linnow, K., Steiger, M., El Jarad, A., Gülker, G. (2000), In: Kwiatkowski D, Löfvendahl R, editors. Proceedings of the 10th International Congress on the Deterioration and Conservation of Stone, ICOMOS, Stockholm, p. 187–194.

[49] Bläuer Böhm, C., Küng, A., Zehnder, K. (2001): Salt Crystal Intergrowth in Efflorescence on Historic Buildings, *Chimia 2001*, 55, 996–1001.

[50] Campos-Suñol, M. J., Domínguez - Vidal, A., Ayora-Cañada, M. J., De la Torre-López, M. J. Renaissance patinas in Ubeda (Spain): mineralogic, petrographic and spectroscopic study, *Analytical and Bioanalytical Chemistry*, 391, 1039–1048.